

## EFFECTS OF PRESSURE STRESS WORK AND THERMAL RADIATION ON FREE CONVECTION FLOW AROUND A SPHERE EMBEDDED IN A POROUS MEDIUM WITH NEWTONIAN HEATING

by

**Elsayed M. A. ELBASHBESHY<sup>a</sup>, Nabil T. M. ELDABE<sup>b</sup>,  
Ismail K. YOUSSEF<sup>a</sup>, and Ahmed M. SEDKI<sup>a,c\*</sup>**

<sup>a</sup> Mathematics Department, Faculty of Science, Ain Shams University, Cairo, Egypt  
<sup>b</sup> Mathematics Department, Faculty of Education, Ain Shams University, Cairo, Egypt  
<sup>c</sup> Mathematics Department, Faculty of Science, Jazan University, Jazan, Saudi Arabia

Original scientific paper  
<https://doi.org/10.2298/TSCI150601207E>

*The effects of pressure stress work and thermal radiation on free convection flow around a sphere embedded in a porous medium with Newtonian heating is considered. The basic equations of boundary-layer are transformed into a non-dimensional form and reduced to non-linear system of partial differential equations and solved numerically using an implicit finite difference technique with Newtons linearization method. Comparisons with previously published work are performed and excellent agreement is obtained. Numerical results have been shown graphically and tabular forms for some selected values of parameters set consisting of radiation parameter, pressure stress work parameter, Newtonian heating coefficient, and Prandtl number.*

Key words: *porous medium, free convection, pressure work, thermal radiation, Newtonian heating*

### Introduction

Free convection boundary-layer flow around a sphere in a porous medium represents an important problem, which is related to numerous engineering applications. Such problems are spherical storage tanks, packed beds of spherical bodies, and nuclear waste disposal. Many researchers have studied the problems of free convection boundary-layer flow over a sphere. Amongst them Nazar *et al.* [1] have studied free convection boundary-layer on an isothermal sphere in micropolar fluid. Akhter and Alim [2] studied the effects of radiation on natural convection flow around a sphere with uniform surface heat flux. Alam *et al.* [3] studied the viscous dissipation effects with MHD natural convection flow on a sphere in the presence of heat generation. Chen and Mucogle [4, 5] studied mixed convection over a sphere with uniform surface temperature and uniform surface heat flux. The thermal radiation effects on the natural convection flow are important in various engineering applications and new modern technology, such as in advanced power plants for nuclear rockets, high speed flights, satellites and space vehicles, and processes involving high temperatures. At a high temperature the presence of thermal radiation affects on the distribution of temperature in the boundary-layer, which in turn affects on the heat transfer at the wall. In such problems the effects of convective and thermal radiation must be simultaneously investigated as shown in Cheng and Ozisik [6] and Ozisik [7].

\* Corresponding author, e-mail: a.m.sedki@hotmail.com

Azzam [8] reported the radiation effect on the MHD mixed free-forced convective flow past a semi-infinite moving vertical plate for high temperature difference. Molla *et al.* [9] investigated the radiation effect on free convection laminar flow from an isothermal sphere. Chamkha and Al-Mudhaf [10] studied the heat and mass transfer by natural convection from a permeable sphere in the presence of thermal radiation. The pressure work effect plays an important role in free convection in various devices which are subjected to large deceleration or which operate at high rotational speed and also in strong gravitational field processes on large scales and in geological processes. Akhter and Alim [11] and Miraj *et al.* [12] studied the effects of pressure work and radiation on natural convection flow around a sphere with heat generation. El-Kabeir *et al.* [13] studied the natural convection from a permeable sphere embedded in porous medium due to thermal dispersion. The heat transfer with Newtonian heating occurs in many important engineering devices, for example in heat exchanger where the conduction in solid tube wall is greatly affected by the convection in the fluid flow around it. The Newtonian heating condition was pioneered by Merkin [14] for the free convection boundary-layer flow over a vertical flat plate. However, due to its importance in numerous practical applications in various engineering devices, several researchers are getting interested to investigate the Newtonian heating condition in different heat transfer problems. Pop *et al.* [15] considered the free convection boundary-layer flow along a vertical surface in a porous medium with Newtonian heating. Chaudhary and Jain [16] studied unsteady free convection boundary-layer flow past an impulsively started vertical surface with Newtonian heating. Recently, Salleh *et al.* [17, 18] studied the effect of Newtonian heating on mixed and free convection boundary-layer flow on a solid sphere in a micropolar fluid.

To our best of knowledge, the combined effects of the pressure stress work and thermal radiation on free convection flow around a solid sphere with Newtonian heating has not been studied yet and the present work is proposed to fill this gap. Motivated by the previously mentioned studies, therefore, the aim of the present paper is to study the effects of pressure stress work and thermal radiation on free convection boundary-layer flow around a sphere embedded in a porous medium with Newtonian heating.

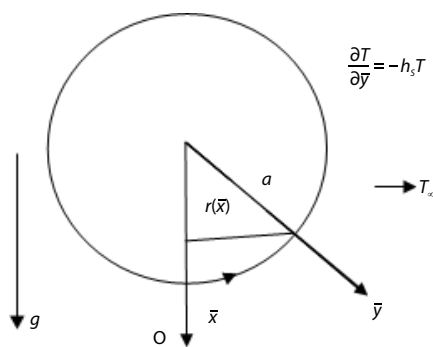


Figure 1. The physical model and co-ordinate system

### Formulation of the problem

Consider the steady 2-D free convection boundary-layer flow of an incompressible viscous fluid around a sphere embedded in a fluid saturated porous medium with pressure stress work and thermal radiation, fig. 1. In this analysis  $T_\infty$  being the ambient temperature of the fluid and  $T$  is the temperature of the fluid within the boundary-layer. Under the Boussinesq and the boundary-layer approximations, the basic dimensional equations of the flow are:

$$\frac{\partial}{\partial \bar{x}}(r\bar{u}) + \frac{\partial}{\partial \bar{y}}(r\bar{v}) = 0 \quad (1)$$

$$\bar{u} \frac{\partial \bar{u}}{\partial \bar{x}} + \bar{v} \frac{\partial \bar{u}}{\partial \bar{y}} = \nu \left( \frac{\partial^2 \bar{u}}{\partial \bar{y}^2} \right) + g\beta(T - T_\infty) \sin\left(\frac{\bar{x}}{a}\right) - \frac{\nu}{k} \bar{u} \quad (2)$$

$$\bar{u} \frac{\partial T}{\partial \bar{x}} + \bar{v} \frac{\partial T}{\partial \bar{y}} = \frac{K}{\rho C_p} \frac{\partial^2 T}{\partial \bar{y}^2} + \frac{T\beta}{\rho C_p} \bar{u} \frac{\partial P}{\partial \bar{x}} - \frac{1}{\rho C_p} \frac{\partial q_r}{\partial \bar{y}} \quad (3)$$

The boundary conditions for the velocity components and the temperature are:

$$\bar{u} = 0, \quad \bar{v} = 0, \quad \text{and} \quad \frac{\partial T}{\partial \bar{y}} = h_s T \quad \text{on} \quad \bar{y} = 0, \quad \bar{x} > 0 \quad (4)$$

$$\bar{u} \rightarrow 0 \quad \text{and} \quad T \rightarrow T_\infty \quad \text{as} \quad \bar{y} \rightarrow \infty, \quad \bar{x} > 0 \quad (5)$$

where  $\bar{x}, \bar{y}$ , are the dimensional co-ordinates along and normal to the tangent of the surface,  $\bar{u}, \bar{v}$  – the velocity components parallel to,  $\bar{x}, \bar{y}$ , not rotate relative to the surface,  $r(\bar{x})$  – the radial distance from the symmetric axis to the surface of the sphere,  $g$  – the acceleration due to gravity,  $k$  – the permeability of the medium,  $\nu = \mu/\rho$  – the kinematic viscosity where  $\rho$  is the density and  $\mu$  – the dynamic viscosity of the fluid,  $T_\infty$  – the ambient temperature of the fluid,  $\beta$  – the coefficient of thermal expansion,  $K$  – the thermal conductivity of the fluid, and  $q_r$  – the radiation heat flux parameter. The radiatio heat flux  $q_r$  is simplified by the Rosseland diffusion approximation, which has been extensively used (see Molla *et al.* [9]), as:

$$q_r = -\frac{4\sigma}{3(a_r + \sigma_s)} \frac{\partial T^4}{\partial \bar{y}} \quad (6)$$

where  $a_r$  is the Rosseland mean absorption coefficient,  $\sigma_s$  – the scattering coefficient, and  $\sigma$  – the Stefan-Boltzmann constant. Now we introduce the following non-dimensional variables:

$$x = \frac{\bar{x}}{a}, \quad y = \frac{\bar{y}}{a} \text{Gr}^{1/4}, \quad u = \frac{\rho a}{\mu_\infty} \text{Gr}^{-1/2} \bar{u}, \quad (7)$$

$$v = \frac{\rho a}{\mu_\infty} \text{Gr}^{-1/4} \bar{v}, \quad \theta = \frac{T - T_\infty}{T_w - T_\infty}, \quad \text{Gr} = \frac{g\beta(T_w - T_\infty)a^3}{\nu_\infty^2}$$

where  $\theta$  is the non-dimensional temperature,  $\nu_\infty$  – the reference kinematic viscosity, and Gr – the Grashof number. Substituting variables in eq. (7) into eqs. (1)-(3), the non-dimensional forms of the governing equations are:

$$\frac{\partial}{\partial x}(ru) + \frac{\partial}{\partial y}(rv) = 0 \quad (8)$$

$$u \frac{\partial u}{\partial x} + v \frac{\partial u}{\partial y} = \frac{\partial^2 u}{\partial y^2} + \theta \sin x - \frac{1}{\text{Da}} u \quad (9)$$

$$u \frac{\partial \theta}{\partial x} + v \frac{\partial \theta}{\partial y} = \frac{1}{\text{Pr}} \left[ \frac{\partial^2 \theta}{\partial y^2} + \frac{4}{3} \text{Rd} \frac{\partial}{\partial y} \left\{ [1 + (\theta_w - 1)\theta]^3 \frac{\partial \theta}{\partial y} \right\} \right] + \varepsilon \left( \frac{1}{\theta_w - 1} + \theta \right) u \quad (10)$$

where Da is the Darcy number, Pr – the Prandtl number, Rd – the radiation parameter or Planck number,  $\varepsilon$  – the pressure stress work parameter, and  $\theta_w$  – the surface heating parameter, which are defined, respectively:

$$\text{Da} = \frac{k\text{Gr}^{1/2}}{a^2}, \quad \text{Pr} = \frac{\mu C_P}{K}, \quad \text{Rd} = \frac{4\sigma T_\infty^3}{K(a_r + \sigma_s)}, \quad \varepsilon = \frac{g\beta a}{C_P}, \quad \theta_w = \frac{T_w}{T_\infty} \quad (11)$$

The boundary conditions can be written in the following non-dimensional forms:

$$u = v = 0, \quad \frac{\partial \theta}{\partial y} = -\chi(\theta + 1) \quad \text{on} \quad y = 0, \quad x > 0 \quad (12)$$

$$u \rightarrow 0 \quad \text{and} \quad \theta \rightarrow 0 \quad \text{as} \quad y \rightarrow \infty, \quad x > 0$$

where  $\chi = a(h_s / k)Gr^{-1/4}$  is the conjugate parameter for the convective boundary condition, it is noticed that when  $\chi = 0$  the sphere surface temperature is constant. The stream function  $\psi(x,y)$  that satisfies the continuity equation is related to the velocity components in the usual way:

$$u = \frac{1}{r} \frac{\partial \psi}{\partial y} \quad \text{and} \quad v = -\frac{1}{r} \frac{\partial \psi}{\partial x} \quad (13)$$

Using boundary-layer approximation, the dimensionless variables for the stream function can be introduced:

$$\psi = x r(x) f(x, y) \quad (14)$$

Substituting in eqs. (6)-(9) to obtain the following equations:

$$\frac{\partial^3 f}{\partial y^3} + \left(1 + \frac{x}{\sin x} \cos x\right) f \frac{\partial^2 f}{\partial y^2} - \left(\frac{\partial f}{\partial y}\right)^2 - \frac{1}{Da} \frac{\partial f}{\partial y} + \theta \frac{\sin x}{x} = x \left( \frac{\partial f}{\partial y} \frac{\partial^2 f}{\partial y \partial x} - \frac{\partial^2 f}{\partial y^2} \frac{\partial f}{\partial x} \right) \quad (15)$$

$$\begin{aligned} & \frac{1}{Pr} \left[ \frac{\partial^2 \theta}{\partial y^2} + \frac{4}{3} Rd \frac{\partial}{\partial y} \left( [1 + (\theta_w - 1)\theta]^3 \frac{\partial \theta}{\partial y} \right) \right] + \left(1 + \frac{x}{\sin x} \cos x\right) f \frac{\partial \theta}{\partial y} + \\ & + \varepsilon x \left( \frac{1}{\theta_w - 1} + \theta \right) \frac{\partial f}{\partial y} = x \left( \frac{\partial f}{\partial y} \frac{\partial \theta}{\partial x} - \frac{\partial \theta}{\partial y} \frac{\partial f}{\partial x} \right) \end{aligned} \quad (16)$$

The boundary conditions finally become:

$$f = \frac{\partial f}{\partial y} = 0 \quad \text{and} \quad \frac{\partial \theta}{\partial y} = -\chi(\theta + 1) \quad \text{at} \quad y = 0, \quad x > 0 \quad (17)$$

$$\frac{\partial f}{\partial y} \rightarrow 0 \quad \text{and} \quad \theta \rightarrow 0 \quad \text{as} \quad y \rightarrow \infty, \quad x > 0 \quad (18)$$

The physical quantities of interest in this problem are shearing stress in terms of the skin friction coefficient and rate of heat transfer which can be written in non-dimensional form:

$$C_f = \frac{a^2 Gr^{3/4}}{\mu \nu} \tau_w \quad \text{and} \quad Nu = \frac{a Gr^{1/4}}{k(T_w - T_\infty)} q_w \quad (19)$$

Here  $\tau_w$  is the shearing stress and  $q_w$  is the heat flux at the surface defined, respectively:

$$\tau_w = \mu \left( \frac{\partial \bar{u}}{\partial y} \right)_{y=0} \quad \text{and} \quad q_w = (q_c + q_r)|_{y=0} \quad (20)$$

where  $q_c = -K[\partial T / \partial y]$  is the conduction heat flux,  $K$  – the thermal conductivity of the fluid, and  $q_r$  is the radiation heat flux. Using the non-dimensional variables in eqs. (7) and (14) in eq. (19), we get:

$$C_f = x \left[ \frac{\partial^2}{\partial y^2} f(x, y) \right]_{y=0} \quad \text{and} \quad Nu = - \left[ \left( 1 + \frac{4}{3} Rd \theta_w^3 \right) \frac{\partial}{\partial y} \theta(x, y) \right]_{y=0} \quad (21)$$

## Results and discussion

The non-linear system of PDE (15) and (16) subjected to the boundary condition and (17) and (18) is solved numerically by using an implicit finite difference method together with Newtons linearization scheme which was first introduced by Keller [19] and described by Cebeci and Bradshaw[19]. The computations were performed using non-uniform grid in the y-direction and it was defined by  $y_i = \sin h[(j - 1) / 100]$  where  $j = 1, 2, \dots, 170$  and  $\Delta x = 0.01$ .

The results are obtained in terms of velocity profiles, temperature distributions, skin friction coefficient, and the rate of heat transfer and presented graphically and tabular form for selected values of the thermal radiation parameter, Darcy number, Newtonian heating parameter, and the pressure stress work. In order to verify the accuracy of the present method, the present results are compared with those reported by Salleh *et al.* [18]. It is found that the agreement between the previously published results with the present ones is very good, as shown in the tab. 1.

**Table 1. Comparisons of the present numerical results of  $C_f$  for the  $Pr = 0.7$ , 1, and 7.0 without effect of the thermal radiation-conduction, stress work, and porous medium with those obtained by Salleh *et al.* [18]**

$x$	Pr = 0.7		Pr = 1.0		Pr = 7.0	
	Salleh <i>et al.</i> [18]	Present	Salleh <i>et al.</i> [18]	Present	Salleh <i>et al.</i> [18]	Present
0	0.0000	0.0000	0.0000	0.0000	0.0000	0.0000
$\pi/18$	2.8206	2.8219	1.8939	1.8941	0.2909	0.2913
$\pi/9$	5.7090	5.7103	3.8939	3.8945	0.5854	0.5871
$\pi/6$	8.7332	8.7329	5.8418	5.8421	0.8785	0.8789
$2\pi/9$	11.5864	11.5863	7.7431	7.7429	1.1618	1.1614
$5\pi/18$	14.3102	14.3105	9.5616	9.5621	1.4186	1.4190
$\pi/3$	16.7934	16.7937	11.2211	11.2209	1.6778	1.6781
$7\pi/18$	19.1415	19.1413	12.7925	12.7931	1.9052	1.9056
$4\pi/9$	21.2356	21.2358	14.1966	14.1963	2.1172	2.1173
$\pi/2$	23.0291	23.0294	15.4035	15.4041	2.3029	2.3034
$5\pi/9$	24.4695	24.4689	16.3780	16.3878	2.4569	2.4570
$11\pi/18$	25.4947	25.4944	17.0803	17.0805	2.5741	2.5745
$2\pi/3$	26.0269	26.0273	17.4585	17.4588	2.6466	2.6571

The effect of radiation parameter on skin friction and rate of heat transfer, Nu, are considered in tab. 2 with  $Pr = 0.7$ ,  $\theta_w = 1.2$ ,  $Da = 10$ ,  $\chi = 1.0$ , and  $\varepsilon = 0.1$ . From tab. 2, it can be seen that an increase in radiation parameter causes an increase in both the skin friction coefficient and the Nusselt number. That is due to the fact that an increase in the values of  $Rd$  leads to more interaction of radiation with momentum transfer and so thermal boundary layers. We found at  $x = \pi/6$  that the skin friction increases by 0.44% and the Nusselt number increases by 130.25% while  $Rd$  increases from 1.0 to 3.0.

The effects Prandtl number on skin friction and Nusselt number are considered in tab. 3 with  $Rd = 1.0$ ,  $\theta_w = 1.2$ ,  $Da = 10$ , and  $\varepsilon = 0.1$ . From tab. 3. it is found that the skin friction coefficient decreases but the Nusselt number increases with the increment of Prandtl number. We noted at  $x = \pi/6$  that the skin friction coefficient decreases by 4.43% and the Nusselt number increases by 33.17%, while Prandtl number increases from 0.72 to 7.0. It is known that the fluids which have large values of Prandtl number are less thermally conductive and the thermal boundary-layer of the conducted fluids around the surface of the heated sphere becomes thinner with a high temperature gradient which increases the surface rate of heat transfer but decreases skin friction coefficient.

**Table 2. The  $C_f$  and Nu values for various values of  $Rd$  while  $\chi = 1.0$ ,  $\varepsilon = 0.1$ ,  $Da = 10$ ,  $Pr = 0.7$ , and  $\theta_w = 1.2$** 

$x$	$Rd = 1$		$Rd = 2.0$		$Rd = 3$	
	$C_f$	Nu	$C_f$	Nu	$C_f$	Nu
0	0.00	9.17556	0.00	15.07628	0.00	21.03724
$\pi/18$	1.72196	9.160263	1.727878	15.06308	1.729836	21.02454
$\pi/9$	3.409141	9.140245	3.420692	15.04593	3.424513	21.00839
$\pi/6$	5.027081	9.115567	5.043816	15.02498	5.049351	20.98853
$2\pi/9$	6.542363	9.08633	6.563687	14.99999	6.570742	20.96512
$5\pi/18$	7.923126	9.052567	7.948312	14.97132	7.956648	20.93815
$\pi/3$	9.13942	9.014247	9.167632	14.93882	9.176972	20.90758
$7\pi/18$	10.16351	8.971218	10.19383	14.90232	10.20386	20.87326
$4\pi/9$	10.97002	8.923131	11.00144	14.8615	11.01185	20.83487
$\pi/2$	11.53582	8.869287	11.5673	14.8157	11.57773	20.79176

**Table 3. The  $C_f$  and Nu values for various values of  $Pr$  while  $Rd = 1.0$ ,  $\chi = 1.0$ ,  $\varepsilon = 0.1$ ,  $Da = 10$ , and  $\theta_w = 1.2$** 

$x$	$Pr = 0.72$		$Pr = 1.7$		$Pr = 7.0$	
	$C_f$	Nu	$C_f$	Nu	$C_f$	Nu
0	0.00	9.18465	0.00	9.643763	0.00	12.69916
$\pi/18$	1.721784	9.168919	1.712714	9.607274	1.641182	12.57113
$\pi/9$	3.408808	9.148341	3.391366	9.559106	3.252926	12.38769
$\pi/6$	5.0266	9.122952	5.001834	9.499302	4.804014	12.14928
$2\pi/9$	6.541767	9.09288	6.511028	9.428044	6.263842	11.8567
$5\pi/18$	7.922446	9.05815	7.887333	9.345727	7.602886	11.50825
$\pi/3$	9.138692	9.018733	9.100992	9.252323	8.792698	11.11033
$7\pi/18$	10.16277	8.974475	10.12438	9.147675	9.806292	10.66399
$4\pi/9$	10.96931	8.925017	10.93216	9.03123	10.61826	10.17131
$\pi/2$	11.53517	8.869649	11.50115	8.901759	11.20465	9.635026

The effect of pressure stress work on skin friction coefficient, and rate of heat transfer Nu are considered in tab. 4 with  $Pr = 0.7$ ,  $\theta_w = 1.2$ ,  $Rd = 1.0$ ,  $Da = 10$ , and  $\chi = 1.0$ . From tab. 4, it can be seen that an increase in the stress work parameter results an increase in the skin friction coefficient on another hand it decreases the Nusselt number. We can see from tab. 3 that the skin friction coefficient increases by 0.14% and the Nusselt number decreases by 2.95 % at  $x = \pi/6$  while  $\varepsilon$  increases from 0.1 to 0.8.

The effects Darcy number on skin friction coefficient and rate of heat transfer Nu are considered in tab. 5 with  $Pr = 0.7$ ,  $\theta_w = 1.2$ ,  $Rd = 1.0$ ,  $\varepsilon = 0.1$ , and  $\chi = 1.0$ . It can be seen that the increasing of the Darcy number implies increasing in both the skin friction coefficient and

**Table 4. The  $C_f$  and Nu values for various values of  $\varepsilon$  while  $\chi = 1.0$ ,  $Rd = 1.0$ ,  $Da = 10$ ,  $Pr = 0.7$ , and  $\theta_w = 1.2$**

$x$	$\varepsilon = 0.1$		$\varepsilon = 0.5$		$\varepsilon = 0.8$	
	$C_f$	Nu	$C_f$	Nu	$C_f$	Nu
0	0.00	9.17556	0.00	9.175546	0.00	9.175535
$\pi/18$	1.72196	9.160263	1.722426	9.108632	1.722776	9.069809
$\pi/9$	3.409141	9.140245	3.410989	9.037262	3.412373	8.959687
$\pi/6$	5.027081	9.115567	5.031158	8.961989	5.034217	8.846267
$2\pi/9$	6.542363	9.08633	6.549444	8.883089	6.554762	8.729724
$5\pi/18$	7.923126	9.052567	7.933853	8.801049	7.941911	8.610967
$\pi/3$	9.13942	9.014247	9.154281	8.71619	9.165447	8.490601
$7\pi/18$	10.16351	8.971218	10.18281	8.628718	10.19732	8.369102
$4\pi/9$	10.97002	8.923131	10.99386	8.538643	11.01178	8.246764
$\pi/2$	11.53582	8.869287	11.56406	8.445674	11.58529	8.12361

the Nusselt number. We noted from tab. 5 that the skin friction coefficient increases by 91.91% and the Nusselt number increases by 1.6% at  $x = \pi/6$  while Darcy number increases from 0.1 to 10.0. That is due to the fact that the relationship between the Darcy number and porous medium effect is inverse relationship and the presence of a porous medium represents a resistance to flow which results the slowing of fluid flow and heat transfer and then decreases the rate of heat transfer and skin friction coefficient.

**Table 5. The  $C_f$  and Nu values for various values of  $Da$  while  $\chi = 1.0$ ,  $Rd = 1.0$ ,  $\varepsilon = 0.1$ ,  $Pr = 0.7$  and  $\theta_w = 1.2$**

$x$	$Da = 0.1$		$Da = 1$		$Da = 10$	
	$C_f$	Nu	$C_f$	Nu	$C_f$	Nu
0	0.00	9.005475	0.00	9.151776	0.00	9.17556
$\pi/8$	0.907825	8.997654	1.589756	9.137446	1.72196	9.160263
$\pi/9$	1.789496	8.986392	3.14514	9.118458	3.409141	9.140245
$\pi/6$	2.619479	8.971845	4.632137	9.095008	5.027081	9.115567
$2\pi/9$	3.373552	8.954213	6.017816	9.066826	6.542363	9.08633
$5\pi/18$	4.029436	8.933927	7.270854	9.034382	7.923126	9.052567
$\pi/3$	4.567382	8.911308	8.361936	8.997557	9.13942	9.014247
$7\pi/18$	4.970721	8.886785	9.264119	8.95627	10.16351	8.971218
$4\pi/9$	5.226372	8.860851	9.953053	8.910285	10.97002	8.923131
$\pi/2$	5.325284	8.834079	10.40704	8.859091	11.53582	8.869287

In tab. 6, the values of  $C_f$  and Nu are given for different values of the Newtonian heating parameter while  $\varepsilon = 0.1$ ,  $Da = 10$ ,  $Rd = 1.0$ ,  $Pr = 0.7$ , and  $\theta_w = 1.2$ . Here we found that the values of skin friction coefficient  $C_f$  increase at the different positions of  $x$  for increasing values of the Newtonian heating parameter. The skin friction coefficient is increased by 3094.81% as Newtonian heating parameter changes from 0.01 to 1.0 at  $x = \pi/6$ . Furthermore, it is seen that

the numerical values of the Nu increase for increasing values of Newtonian heating parameter. The rate of local Nusselt number is increased by 1554.28% at position  $x = \pi/6$  as Newtonian heating parameter changes from 0.01 to 1.0.

**Table 6.** The  $C_f$  and Nu values for various values of  $\chi$  while  $\varepsilon = 0.10$ ,  $Rd = 1.0$ ,  $Da = 10$ ,  $Pr = 0.7$ , and  $\theta_w = 1.2$

$x$	$\chi = 0.1$		$\chi = 0.5$		$\chi = 1$	
	$C_f$	Nu	$C_f$	Nu	$C_f$	Nu
0	0.00	0.5652026	0.00	3.735442	0.00	9.17556
$\pi/18$	0.05421395	0.5605906	0.4339737	3.715599	1.72196	9.160263
$\pi/9$	0.1071549	0.5558059	0.8590297	3.691032	3.409141	9.140245
$\pi/6$	0.1573519	0.5510297	1.265845	3.661947	5.027081	9.115567
$2\pi/9$	0.2033916	0.546257	1.645387	3.628569	6.542363	9.08633
$5\pi/18$	0.2439318	0.5416522	1.989009	3.591258	7.923126	9.052567
$\pi/3$	0.2777443	0.5373347	2.288726	3.549834	9.13942	9.014247
$7\pi/18$	0.3037451	0.5334247	2.537177	3.504621	10.16351	8.971218
$4\pi/9$	0.3210262	0.5300417	2.727767	3.455739	10.97002	8.923131
$\pi/2$	0.3288863	0.5273022	2.854734	3.403231	11.53582	8.869287

The effects of the Prandtl number with  $Rd = 1.0$ ,  $Da = 10$ ,  $\theta_w = 1.2$ ,  $\varepsilon = 0.1$ , and  $\chi = 0.1$  at  $x = \pi/6$  on the velocity and the temperature profiles are indicated in figs. 2(a) and 2(b). It can be seen that the increasing values of Prandtl number leads to the decrease in the velocity profiles. We observed that at each value of the Prandtl number, the velocity profile has a maximum value within the boundary-layer. The maximum values of the velocity are 0.6997, 0.6007, and 0.4161 at  $y = 0.81$ , 0.75 and 0.63 for  $Pr = 0.7$ , 1.7, and 7.0, respectively. The maximum velocity decreases by 40.53% as Prandtl number increases from 0.7 to 7.0. From figure 2(b), we noted that the temperature profiles decrease with the increasing values of Prandtl number. That is due

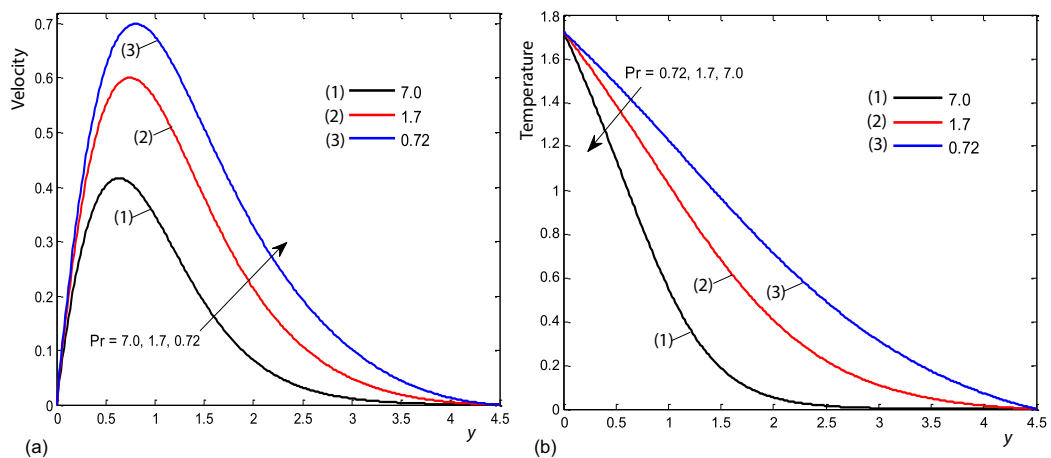


**Figure 2.** (a) Velocity profiles (b) temperature distributions for  $Pr = 0.72, 1.7, 7.0$  while  $\varepsilon = 0.1$ ,  $Da = 10$ ,  $Rd = 1.0$ ,  $\theta_w = 1.2$ , and  $\chi = 0.1$  at  $x = \pi/6$



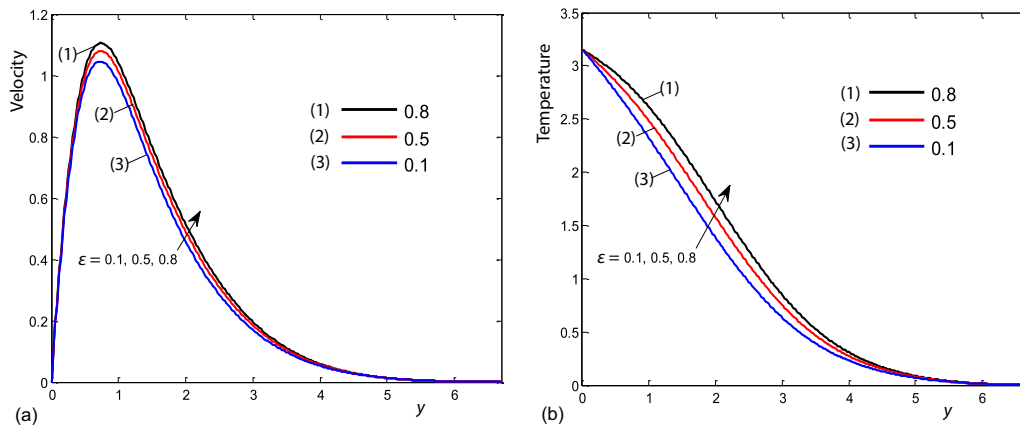


**Figure 3. (a) Velocity profiles (b) temperature distributions for  $\varepsilon = 0.1, 0.5, 0.8$  while  $Pr = 0.72, Da = 10, Rd = 1.0, \theta_w = 1.2,$  and  $\chi = 0.1$  at  $x = \pi/6$**

to the Prandtl number is the ratio of viscous force and thermal force. Thus, the increasing of Prandtl number increases viscosity and decreases the thermal action of the fluid and hence decreases the velocity and the temperature of the fluid. Also, we note that the thickness of the thermal boundary-layer decreases as Prandtl number increases. The effects of pressure stress work  $\varepsilon$  on the velocity and temperature distributions are displayed in figs. 3(a) and 3(b) while  $Pr = 0.72, Da = 10, Rd = 1.0, \theta_w = 1.2,$  and  $\chi = 0.1$  at  $x = \pi/6$ . We observed in these figures that the velocity and temperature profiles increase with the increasing of pressure stress work. We observed that at each value of the pressure stress work parameter, the velocity profile has a maximum value within the boundary-layer. The maximum values of the velocity are 1.045, 1.079, and 1.106 at  $y = 0.74$  for  $\varepsilon = 0.1, 0.5, 0.8,$  respectively. The maximum velocity increases by 5.84% as  $\varepsilon$  increases from 0.1 to 0.8. Figures 4(a) and 4(b), illustrate the velocity and temperature distributions against  $y$  for different values of Darcy number while  $Pr = 0.7, \varepsilon = 0.1, Rd = 1.0, \theta_w = 1.2,$  and  $\chi = 0.1$  at  $x = \pi/6$ . It can be seen that an increasing of Darcy number increases the velocity distributions while decreases the temperature distribution. It is due to that the presence of porous medium causes higher restriction to the fluid, which reduces velocity and enhanced the temperature. We observed that for selected value of the Darcy number, the velocity profile has

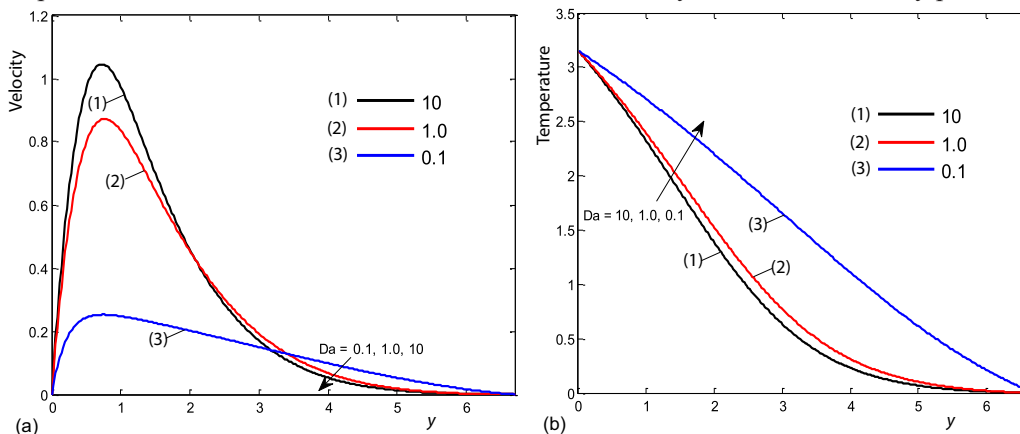


**Figure 4. (a) Velocity profiles (b) temperature distributions for  $Da = 0.1, 1.0, 10$  while  $Pr = 0.72, \varepsilon = 0.1, Rd = 1.0, \theta_w = 1.2,$  and  $\chi = 0.1$  at  $x = \pi/6$**

a maximum value within the boundary-layer. The maximum values of the velocity are 0.2527, 0.8721, and 1.045 at  $y = 0.74, 0.76, 0.73$  for  $Da = 0.1, 1.0,$  and  $10,$  respectively, with  $Rd = 1.0,$   $Pr = 0.7,$   $\theta_w = 1.2,$   $\varepsilon = 0.1,$  and  $\chi = 0.1.$  It is found that the maximum velocity increases by 313.53% as Darcy number increases from 0.1 to 10.0. The effects of Newtonian heating coefficient with  $Pr = 0.7,$   $Rd = 1.0,$   $\theta_w = 1.2,$   $Da = 10,$  and  $\varepsilon = 0.10$  at  $x = \pi/6$  on the velocity and temperature distributions are displayed in figs. 5(a) and (b). It is observed that the velocity and temperature profile increase with the increasing of Newtonian heating parameter.

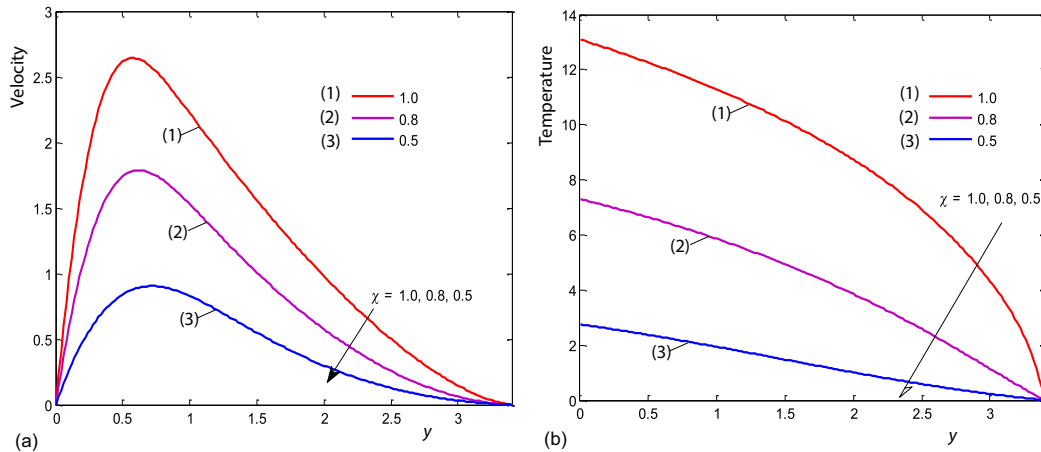


**Figure 5. (a) Velocity profiles (b) temperature distributions for  $\chi = 0.5, 0.8, 1.0$  while  $Da = 10, Pr = 0.7, \varepsilon = 0.1, Rd = 1.0,$  and  $\theta_w = 1.2$**

We observed that at each value of the Newtonian heating parameter the velocity profile has a maximum value within the boundary-layer. The maximum values of the velocity are 0.9045, 1.786, 2.643 at  $y = 0.72, 0.62, 0.58$  for  $\chi = 0.5, 0.8, 1.0,$  respectively. The maximum velocity increases by 192.21% as  $\chi$  increases from 0.5 to 1.0. Figures 6(a) and 6(b), illustrate the effects of radiation parameter on the velocity and temperature distributions against  $y$  at  $x = \pi/6$  while  $Da = 10, Pr = 0.7, \varepsilon = 0.1, \chi = 0.1,$  and  $\theta_w = 1.2.$  It is observed from fig. 6(a) that the

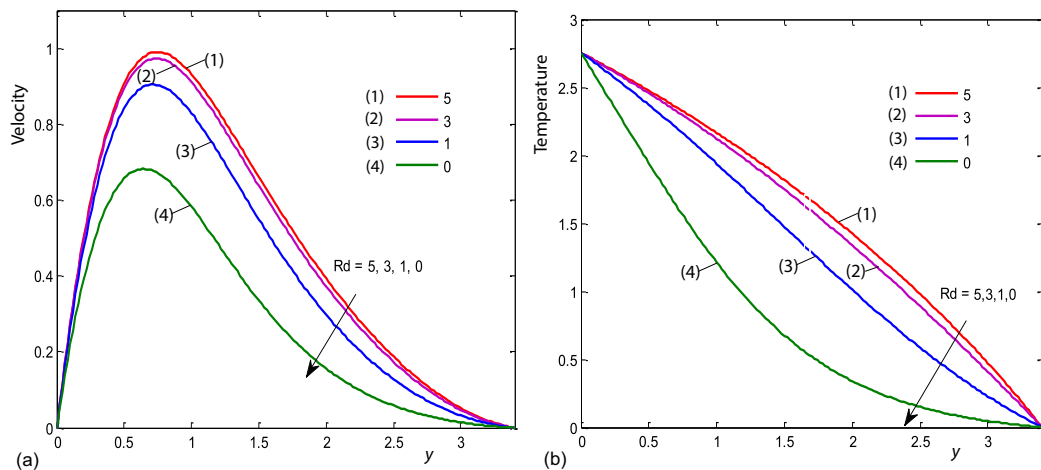


**Figure 6. (a) Velocity profiles (b) temperature distributions for  $Rd = 0, 1, 3, 5$  while  $Da = 10, Pr = 0.7, \varepsilon = 0.1, \chi = 0.5,$  and  $\theta_w = 1.2$  at  $\pi/6$**

increasing of  $Rd$  results an increase in the velocity distributions and for the selected value of  $Rd$  the velocity increases to the peak value as  $y$  increases and finally the velocity approaches to zero (the asymptotic value). The maximum values of velocity are 0.682, 0.9045, 0.973, 0.9901 at  $y = 0.64, 0.72, 0.74$ , for  $Rd = 0.0, 1.0, 3.0, 5.0$ , respectively. It is found that the maximum values of velocity increases by 45.18% as  $Rd$  increases from 0.0 to 5.0. Figure 6(b) displays the temperature profiles against  $y$  which reveals that the temperature increases with increasing radiation parameter  $Rd$ .

### Conclusions

We have investigated the effects of pressure stress work and thermal radiation on free convection flow around a sphere embedded in a porous medium with Newtonian heating. The non-linear system of PDE governing the problem is solved numerically by Keller box method. The results focused on the effects of the radiation parameter, the Darcy number, Newtonian heating, Prandtl number, and stress work parameter on the skin friction coefficient, Nusselt number, velocity profiles, and temperature distributions. From the present investigation the following conclusions may be drawn.

- The values of skin friction coefficient increase for the increment of the parameters, Newtonian heating parameter, the radiation parameter, Darcy number and stress work parameter but the skin friction coefficient decreases with the increasing of Prandtl number.
- The values of Nusselt number increase for the increment of the parameters, Newtonian heating parameter, radiation parameter, Darcy number, and Prandtl number but the Nusselt number decreases with the increasing of the pressure stress work.
- The velocity profiles increase for the increment of the parameters, Newtonian heating parameter, the radiation parameter, Darcy number, and the stress work parameter but the velocity profiles decrease with the increasing of the Prandtl number.
- The temperature distributions increase for the increment of the parameters, Newtonian heating parameter, the radiation parameter, and the stress work parameter but the temperature distributions decrease with the increasing of the parameters Prandtl number and Darcy number.

### Nomenclature

$a$	– radius of the sphere, [m]
$a_r$	– Rosseland mean absorption coefficient, [–]
$C_f$	– local skin friction coefficient, [–]
$C_p$	– specific heat at constant pressure, [Wm <sup>-1</sup> K <sup>-1</sup> ]
Da	– Darcy number, [–]
Gr	– Grashof number, [–]
$g$	– acceleration due to gravity, [ms <sup>-2</sup> ]
$k$	– permeability of the medium, [m <sup>2</sup> ]
$K$	– thermal conductivity of the fluid, [Wm <sup>-1</sup> K <sup>-1</sup> ]
Nu	– local Nusselt number, [–]
Pr	– Prandtl number, [–]
$q_r$	– radiation heat flux parameter, [Km <sup>-2</sup> ]
$r$	– radial distance from the symmetric axis to the surface of the sphere, [m]
$Rd$	– radiation parameter, [–]
$T$	– temperature of the fluid, [K]
$T_w$	– constant temperature at the wall, [K]
$T_\infty$	– temperature of the ambient fluid, [K]

$\bar{u}, \bar{v}$	– fluid velocities along axes directions, [ms <sup>-1</sup> ]
$\bar{x}, \bar{y}$	– axes directions, [m]

#### Greek symbols

$\beta$	– thermal expansion coefficient, [K <sup>-1</sup> ]
$\varepsilon$	– pressure stress work parameter [–]
$\theta$	– dimensionless temperature function, [–]
$\theta_w$	– surface temperature parameter, [–]
$\mu$	– dynamic viscosity of the fluid, [kgm <sup>-1</sup> s <sup>-1</sup> ]
$\nu$	– kinematic viscosity, [m <sup>2</sup> s <sup>-1</sup> ]
$\rho$	– density of the fluid, [kgm <sup>-3</sup> ]
$\sigma$	– Stefan-Boltzmann constant, [–]
$\sigma_s$	– scattering coefficient, [–]
$\tau_w$	– shearing stress, [Nm <sup>-2</sup> ]
$\chi$	– Newtonian heating coefficient, [–]
$\psi$	– stream function, [–]

#### Subscripts

$w$	– wall conditions
$\infty$	– ambient

## References

- [1] Nazar, R., *et al.*, Free Convection Boundary Layer on an Isothermal Sphere in Micropolar Fluid, *Int. Communications in Heat and Mass Transfer*, 29 (2002), 3, pp. 377-386
- [2] Akhter, T., Alim, M. A., Effects of Radiation on Natural Convection Flow around a Sphere with Uniform Surface Heat Flux, *Journal of Mechanical Engineering, Institution of Engineers, Bangladesh*, 39 (2008), 1, pp. 50-56
- [3] Alam, M. M., *et al.*, Viscous Dissipation Effects with MHD Natural Convection Flow on a Sphere in the Presence of Heat Generation, *Non-Linear Analysis: Modeling and Control*, 12 (2007), 4, pp. 447-459
- [4] Chen, T. S., Mucoglu, A., Analysis of Mixed Forced and Free Convection about a Sphere, *Int. J. Heat Mass Transfer*, 20 (1977), 8, pp. 867-875
- [5] Chen, T. S., Mucoglu, A., Mixed Convection about a Sphere with Uniform Surface Heat Flux, *J. Heat Transfer*, 100 (1978), 3, pp. 542-544
- [6] Cheng, E. H., Ozisik, M. N., Radiation with Free Convection in an Absorbing, Emitting and Scattering Medium, *Int. J. Heat Mass Transfer*, 15 (1972), 6, pp. 1243-1252
- [7] Ozisik, M. N., *Radiative Transfer and Interactions with Conduction and Convection*, John Wiley and Sons, New York, USA, 1973
- [8] Azzam, G. A., Radiation Effects on the MHD Mixed Free-Forced Convective Flow Past a Semi Infinite Moving Vertical Plate for High Temperature Differences, *Phys. Scripta*, 66 (2002), 1, pp. 71-76
- [9] Molla, M. M., *et al.*, Radiation Effect on Free Convection Laminar Flow from an Isothermal Sphere, *Communications*, 198 (2011), 12, pp. 1483-1496
- [10] Chamkha, A. J., Al-Mudhaf, A., Simultaneous Heat and Mass Transfer from a Permeable Sphere at Uniform Heat and Mass Fluxes with Magnetic Field and Radiation Effects, *Num. Heat Transfer A*, 46 (2004), 2, pp. 181-198
- [11] Akhter, T., Alim, M. A., Effects of Radiation on Natural Convection Flow around a Sphere with Uniform Surface Heat Flux, *Journal of Mechanical Engineering, Institution of Engineers, Bangladesh*, 39 (2008), 1, pp. 50-56
- [12] Miraj, M., *et al.*, Effects of Pressure Work and Radiation on Natural Convection Flow around a Sphere with Heat Generation, *Int. Communications in Heat and Mass Transfer*, 38 (2011), 7, pp. 911-916
- [13] El-Kabeir, S. M., *et al.*, Natural Convection from a Permeable Sphere Embedded in a Variable Porosity Porous Medium Due to Thermal Dispersion, *Non-Linear Analysis: Modeling and Control*, 12 (2007), 3, pp. 345-357
- [14] Merkin, J. H., Natural-Convection Boundary-Layer Flow on a Vertical Surface with Newtonian Heating, *Int. J. Heat Fluid Flow*, 15 (1994), 5, pp. 392-398
- [15] Pop, I., *et al.*, Asymptotic Solutions for the Free Convection Boundary Layer Flow along a Vertical Surface in a Porous Medium with Newtonian Heating, *Hybrid Methods in Engineering*, 2 (2000), 1, pp. 31-40
- [16] Chaudhary, R., Jain, P., Unsteady Free Convection Boundary Layer Flow Past an Impulsively Started Vertical Surface with Newtonian Heating, *Romanian Journal of Physics*, 51 (2006), 9-10, pp. 911-921
- [17] Salleh, M. Z., *et al.*, Numerical Solutions of Free Convection Boundary Layer Flow on a Solid Sphere with Newtonian Heating in a Micropolar Fluid, *Meccanica*, 47 (2012), 5, pp. 1261-1269
- [18] Salleh, M. Z., *et al.*, Mixed Convection Boundary Layer Flow about A Solid Sphere with Newtonian Heating, *Archives of Mechanics*, 62 (2010), 4, pp. 283-303
- [19] Keller, H. B., Numerical Methods in Boundary Layer Theory, *Annu. Rev. Fluid Mech.*, 10 (1978), Jan., pp. 417-433
- [20] Cebeci, T., Bradshaw, P., *Physical and Computational Aspects of Convective Heat Transfer*, Springer, New York, USA, 1984